EUROPEAN JOURNAL OF CANCER 47 (2011) 600–610

available at www.sciencedirect.com

ScienceDirect

journal homepage: www.ejconline.com

S100A14 regulates the invasive potential of oral squamous cell carcinoma derived cell-lines *in vitro* by modulating expression of matrix metalloproteinases, MMP1 and MMP9

Dipak Sapkota [a,b], *Ove Bruland* [c], *Daniela Elena Costea* [d], *Hallvard Haugen* [a], *Endre N. Vasstrand* [b], *Salah O. Ibrahim* [a,b,*]

[a] *Department of Biomedicine, University of Bergen, Jonas Lies Vei 91, N5009 Bergen, Norway*
[b] *Department of Clinical Dentistry, Periodontology, University of Bergen, Årstadveien 17, N5009 Bergen, Norway*
[c] *Center of Medical Genetics and Molecular Medicine, Haukeland University Hospital, N5021 Bergen, Norway*
[d] *Section of Pathology, The Gade Institute, University of Bergen, N5021 Bergen, Norway*

ARTICLE INFO

Article history:
Received 28 June 2010
Accepted 14 October 2010
Available online 10 November 2010

Keywords:
S100A14
Invasion
MMP
OSCC
Oral cancer

ABSTRACT

Despite the differential expression of S100A14 (a newly identified S100 member) in various human cancers including oral squamous cell carcinomas (OSCCs), its biological role in tumour invasion has not been characterised. The aim of this study was thus to investigate the possible role of S100A14 in OSCC cell invasion. Using immunohistochemistry in normal ($n = 13$), dysplastic ($n = 10$) and OSCC ($n = 16$) archival tissues, S100A14 protein was found to be down-regulated/lost with concomitant membrane to cytoplasmic translocation in OSCCs, especially in the invading tumour islands. These expression data were corroborated by profiling *S100A14* mRNA expression using quantitative RT-PCR (qRT-PCR) in an *in vitro* human OSCC progression model consisting of cell-lines derived from normal ($n = 3$), dysplastic ($n = 3$) and OSCC ($n = 8$) tissues. Employing *in vitro* Matrigel invasion assay, we demonstrated that retroviral vector mediated over-expression of S100A14 resulted in significant decrease in the invasive potential of OSCC derived CaLH3 and H357 cell-lines whereas siRNA mediated knockdown resulted in significant increase in the invasive potential of CaLH3 cell-line. Pathway focused PCR array and validation using qRT-PCR revealed that S100A14 over-expression was associated with down-regulation of *MMP1* and *MMP9* mRNAs in both CaLH3 and H357 cell-lines. Further, S100A14 over-expression was found to be associated with suppression of MMP9 gelatinolytic activity in CaLH3 cell-line. Additionally, an inverse correlation between mRNA expression levels of *MMP1* and *MMP9* with *S100A14* was found in 19 cases of OSCCs. Collectively, these data provide the first evidence for a role of S100A14 protein in regulation of OSCC cell invasion by modulating expression of *MMP1* and *MMP9*.

1. Introduction

Despite ample research and improvement in diagnostic tools and treatment modalities of oral squamous cell carcinoma (OSCC), overall 5 year survival of OSCC patients is poor (<50%) and has remained unchanged for the last three decades.[1] OSCC is a highly aggressive pathological condition and frequently metastasizes to the regional lymph nodes.

* *Corresponding author* at: Department of Biomedicine, University of Bergen, Jonas Lies Vei 91, N5009 Bergen, Norway. Tel.: +47 55 586 423; fax: +47 55 586 360.
E-mail address: Salah.Ibrahim@biomed.uib.no (S.O. Ibrahim).
0959-8049/$ - see front matter
doi:10.1016/j.ejca.2010.10.012

Status of the metastatic involvement of cervical lymph nodes is a major prognostic factor for OSCC patient survival.[2,3] Although the process of tumour cell invasion and metastasis has been suggested to involve a cascade of alterations in cell–cell and cell-extracellular matrix (ECM) interactions and proteolytic degradation of ECM, followed by motility of the cancer cells towards adjacent connective tissue stroma,[4,5] the precise molecular mechanisms remain elusive in OSCC invasion. Hence, a better understanding of the biology of OSCC invasion and identification of key molecules regulating this process are necessary to predict the invasion and metastatic potential of these lesions.

The S100 family is a multifunctional group of EF-hand type calcium binding proteins. Several members of the S100 family have been reported to regulate a number of biological processes like cell growth, cell motility, signal transduction, transcription, cell survival and apoptosis, related to normal development and tumourigenesis.[6,7] Expression of many of the S100 members has been reported to be altered in various human malignancies.[8–11] In addition, several S100 members, namely S100A4[12], S100A2[13], S100P[14] and S100A13[15] have been implicated in tumour invasion and metastasis. Several studies have documented the role of S100 members in regulation of matrix metalloproteinases (MMPs), the key molecules involved in tumour invasion and metastasis.[12,16,17] MMPs are a large family of zinc-dependent proteolytic enzymes that can degrade virtually any components of ECM, thus allowing migration of cancer cells towards adjacent connective tissue.[18,19] Over-expression of several of the MMPs and their association with tumour progression, invasion and metastasis and poor clinical outcomes has been reported in OSCCs.[20,21]

S100A14 protein (previously known as BCMP84, S100A15) is a recently identified member of the S100 family.[22,23] Although differential expression of S100A14 has been reported in different human malignancies including OSCCs,[9,10,22–24] biological properties of this molecule are largely unknown. We have recently identified a role for S100A14 in the regulation of cell proliferation by inducing G1-phase cell cycle arrest in OSCC derived cells (Dr. D. Sapkota, University of Bergen). In the present study we investigated the possible role of S100A14 in invasion of OSCCs. Here, we demonstrate that S100A14 plays an important role in the regulation of invasiveness of OSCC derived cell-lines *in vitro* with concomitant modulation of *MMP1* and *MMP9* mRNA expressions.

2. Materials and methods

2.1. Tissue specimens and immunohistochemistry (IHC)

Immunohistochemical analysis of the S100A14 protein was performed on archival formalin fixed, paraffin embedded tissue specimens of OSCCs ($n = 16$), oral dysplastic lesions (ODL, $n = 10$, all mild dysplastic lesions) and normal human oral mucosa (NHOM, $n = 13$) using Autostainer universal staining system (DAKO-USA, Carpinteria, CA) as described previously.[25] All tissue samples, except seven of the NHOM specimens, were collected from the Department of Oral and Maxillofacial Surgery, Khartoum whereas the remaining seven NHOM specimens were collected from the Department of Surgical Sciences, Section of Otorhinolaryngology, Haukeland University Hospital after informed consent. This study was approved by the Committees for Medical Ethics at Haukeland University Hospital, Norway, and University of Khartoum, Sudan. Grading and staging of the lesions were performed as previously described.[26] Patients' data on clinicopathological variables are presented in supplementary Table S1. For IHC, antigen retrieval was done by microwave treatment in Tris–EDTA buffer, pH 9.0 (DAKO). After blocking with 3% BSA in TBST, rabbit polyclonal anti-human S100A14 primary antibody (10489-1-AP, Proteintech, Chicago, IL, USA, 1:500 dilutions) was applied. After wash, anti-rabbit secondary antibody conjugated with horseradish peroxidase labelled polymer (EnVision System, DAKO) was applied. Presence of antigen was visualised by staining with 3, 30-diaminobenzidine (DAKO), counterstained with haematoxylin (DAKO) and mounted with EuKit mounting medium. Sections incubated with 3% BSA instead of primary antibody served as negative controls.

2.2. IHC evaluation

Tissue sections were examined with a light microscope for the S100A14 staining. IHC evaluation was mainly focused on the invading islands of the cancer cells in the OSCC specimens. S100A14 staining in OSCCs was semi-quantitatively evaluated by manually counting the cells (at least 500 cells were counted in three representative areas, at 400× magnification) expressing either membranous, mixed membranous and cytoplasmic or only cytoplasmic S100A14 protein. Based on the number of positive cells with respect to the sub-cellular localisation of the S100A14, OSCC cases were categorised into three groups: *low* (0–9% positive cells), *moderate* (10–49% positive cells) and *high score* (50–100% positive cells).

2.3. In vitro human OSCC progression model

An *in vitro* OSCC progression model consisting of human cells derived from NHOM (primary cell strains: NOK94, NOK95, NOK108; $n = 3$), ODL (POE9n,[27] D20,[28] DOK[29]; $n = 3$) and OSCC (SCC4,[30] SCC25,[30] H357,[31] VB6,[32] UK1,[33] CA1,[33] 5PT (T. Carey, University of Michigan), CaLH3[34]; $n = 8$) tissues were used in this study. Primary normal oral keratinocytes (NOK) were isolated from NHOM as described previously.[35] Cells were grown in humidified environment with 5% CO_2 at 37 °C in their routine medium as described previously.

2.4. Construction of the S100A14 expression vector and transfection

Human *S100A14* cDNA was subcloned into the pRetroX-IRES-ZsGreen1 retroviral expression vector (Clontech Laboratories, Inc., CA, USA). CaLH3 and H357 cell-lines were infected with retrovirus derived from packaging (Phoenix A) cells, sorted (GFP as a marker), propagated, verified for S100A14 over-expression and used for functional assays. CaLH3 and H357 cells infected with retrovirus with S100A14 insert and retrovirus without S100A14 insert are referred to as 'S100A14-CaLH3 and S100A14-H357', and 'control-CaLH3 and control-H357' cells, respectively.

2.5. S100A14 siRNA and transfection

Following the fast forward transfection protocol, 5 nM of small interfering RNA (siRNA) targeting S100A14 (NM_020672, with sequences: 5′-UCAAGAACUUUCACCAGUA-3′, 5′-GAGAACUCC CUCUGGAAUU-3′, 5′-CAGAGGAUGCUCA GGAAUU-3, 5′-GCUG ACCCCUUCUGAGCUA-3′, L-010723-00-0010, Thermo Fisher Scientific, Lafayette, CO, USA) and HiPerFect transfection reagent (Qiagen) were used for siRNA transfection in CaLH3 cells. Cells were harvested after 24 h of siRNA treatment for total RNA and for Matrigel invasion assay and after 48 h for protein analysis. Cells treated with a non-targeting pool (scrambled) of siRNA (D-001810-10-20, Thermo Fisher Scientific, Lafayette, CO, USA) were used as controls for transfection. CaLH3 cells treated with scrambled and S100A14 siRNA are referred to as 'sc-siRNA' and 'S100A14-siRNA' cells, respectively. Since H357 cell-line does not express detectable amount of endogenous S100A14, siRNA transfection was not carried out for this cell-line.

2.6. In vitro Matrigel invasion assay

The effect of S100A14 on cell invasion was assayed *in vitro* using Matrigel invasion assay as described previously.[36]

2.7. RNA extraction

For the cell-lines used, total RNA was extracted using RNeasy fibrous tissue mini kit protocol (Qiagen Inc., Valencia, CA, USA). Total RNA from 19 cases of OSCCs ($n = 19$) and their pair-wised normal controls were extracted as described previously.[9] DNase I treatment was done following the manufacturer's instructions. Quantity and purity of the extracted RNA was checked using NanoDrop spectrophotometer (NanoDrop technologies, Inc., Wilmington, DE, USA).

2.8. Expression analysis of invasion and metastasis related genes

To examine the invasion and metastasis related genes possibly modulated by S100A14 over-expression, we used the pathway focussed Human ECM and Cell Adhesion molecules RT^2 Profiler™ PCR Array (PAHS-013E, SABiosciences, Frederick, MD, USA) containing primer pairs for 84 genes related to cell adhesion, invasion and metastasis. Total RNA (3 μg) from three biological replicates ($n = 3$, for both control-CaLH3 and S100A14-CaLH3 cells) was converted to first strand cDNA using RT^2 First Strand Kit (C-03, SABiosciences, Frederick, MD, USA) and PCR amplification was performed using the following cycling conditions: 95 °C for 10 min, (95 °C for 15 s, and 60 °C for 1 min) × 40 cycles in ABI Prism Sequence Detector 7900 HT (Applied Biosystems, Foster City, USA). Pre- and post-PCR quality control measures, as recommended by the manufacturer, were strictly followed. Threshold cycle (Ct) was used to calculate $2^{-\Delta Ct}$ value for each gene using PCR Array Data Analysis Web Portal (SABiosciences). $2^{-\Delta Ct}$ values were then exported to microarray data analysis software (J-Express, 2009).[37] For statistical analysis, unsupervised hierarchical clustering and unpaired SAM (significance analysis of microarray)[38] tests were used. Differentially expressed genes with false discovery rate (FDR) = 0 were considered to be significantly modulated genes.

2.9. cDNA synthesis and quantitative RT-PCR (qRT-PCR)

Following manufacturers' instructions, total RNA (600–900 ng) was converted to cDNA using High-Capacity cDNA Archive Kit system (Applied Biosystems, Foster City, CA, USA). All qRT-PCR amplifications were performed on ABI Prism Sequence Detector 7900 HT (Applied Biosystems, Foster City, USA) as described previously.[9] TaqMan assay for *S100A14* (Hs00221080_m1) was used to profile *S100A14* mRNA in the *in vitro* OSCC progression model and to verify knock-down of *S100A14* mRNA in the S100A14-siRNA cells. SYBR green based qRT-PCR (using the same primer pairs which were used for the construction of S100A14 expression vector) was performed to verify the over-expression of *S100A14* in the S100A14-CaLH3 and S100A14-H357 cells. PCR array data were independently validated by performing qRT-PCR using TaqMan assays for *MMP1* (Hs00233958_m1) and *MMP9* (Hs00957562_m1). *GAPDH* (Hs99999905_m1) was used as an endogenous control. Both relative standard curve and comparative $2^{-\Delta\Delta Ct}$ methods[39] were used to quantify the relative mRNA expression.

2.10. Correlation analysis between S100A14, MMP1 and MMP9 mRNA expression levels in OSCCs

Expression of *S100A14*, *MMP1* and *MMP9* mRNA levels were examined in 19 cases of OSCCs and their pair-wised normal controls by using qRT-PCR as described above. OSCC/normal control ratios of the normalised (normalised with the mRNA expression of *GAPDH*) mRNA levels of both *MMP1* and *MMP9* were then correlated with the *S100A14* mRNA ratios (OSCC/normal control).

2.11. Gelatin zymography

Concentrated serum free conditioned media were used in SDS–PAGE gelatin-substrate zymography (161-1167, Bio-Rad laboratories, Hercules, CA, USA) to detect the activity of MMP9 as described elsewhere.[40] Conditioned serum-free medium from THP-1 cells was used as positive control.

2.12. Western blot

Forty μg of protein was resolved in 12% Tris–HCl gel (161–1156, Bio-Rad laboratories, Hercules, CA, USA) and immunoblotted with polyclonal rabbit anti human-S100A14 (10489-1-AP, Proteintech, Chicago, IL, USA, 1:1000 dilutions) following standard western blot protocol. Anti-GAPDH (ab 9484, Abcam, Cambridge, UK, 1:5000 dilutions) was used as a loading control. Blots were visualised using enhanced chemiluminescence (Supersignal® West pico or Supersignal® West femto; Pierce Biotechnology, Rockford, IL, USA) and images were detected on a KODAK Image Station 2000R (Eastman Kodak Company, Rochester, NY, USA).

2.13. Statistics

Data are expressed as mean ± standard error of the mean (SEM) or standard deviation (SD). Statistical analysis with one-way analysis of variance (ANOVA) with Bonferroni *post-hoc* tests, Student's-t test and Spearman's correlation test were performed using GraphPad Prism software version 3.00 for Windows (GraphPad Software, San Diego California USA, www.graphpad.com), with the level of significance set at 5%.

3. Results

3.1. S100A14 is strongly expressed at the cell membrane of NHOM epithelial cells, but weakly expressed and with membrane-cytoplasmic switch in the invading OSCC cells

All NHOM tissues showed a strong membranous expression of S100A14 protein confined mainly to the epithelial cells (Fig. 1A). Few scattered cells in the epithelium showed a

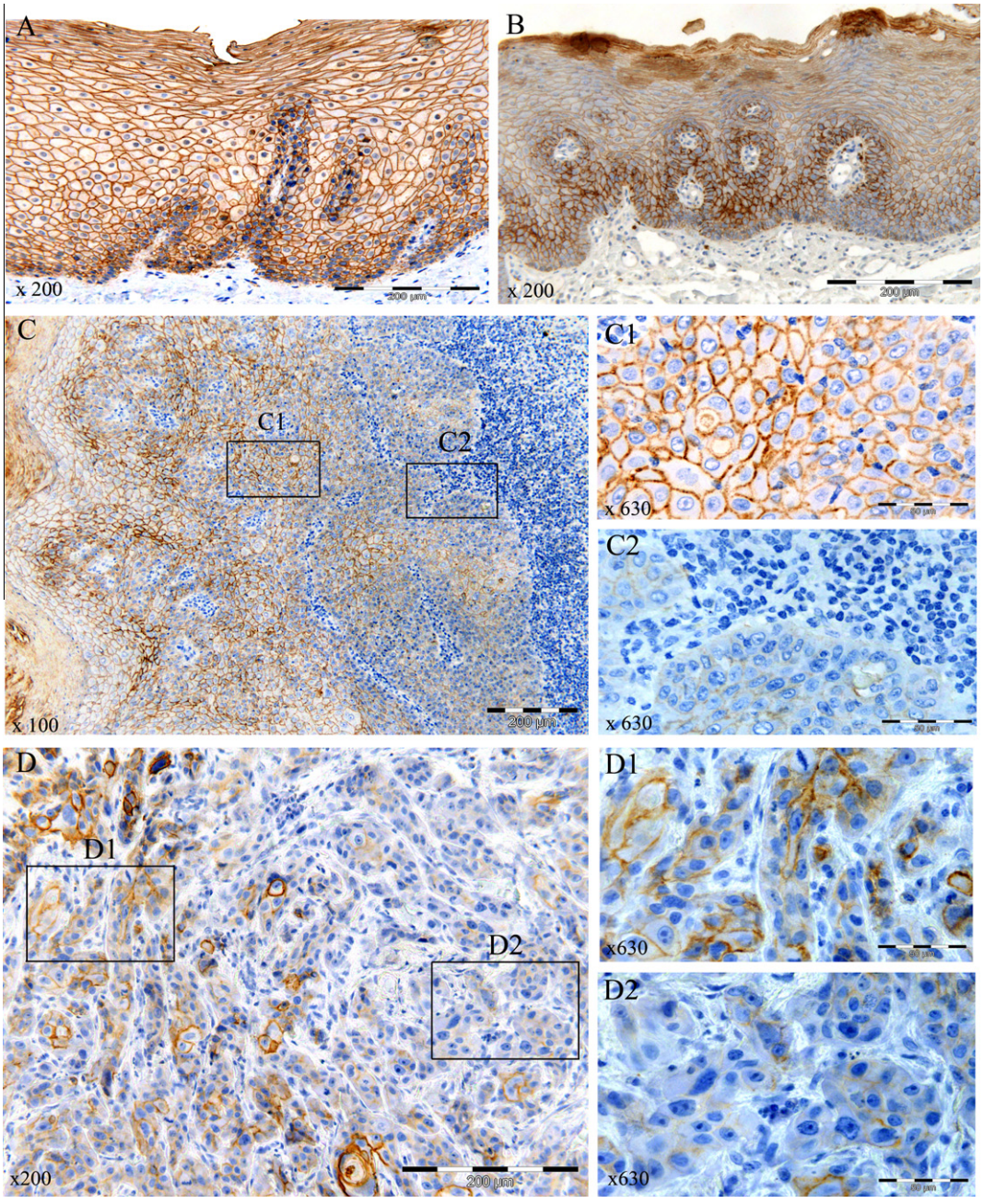

Fig. 1 – Expression and sub-cellular localisation of the S100A14 protein in NHOM, ODL and OSCC. Representative NHOM (A) and ODL (B) specimens showing, respectively, strong and weak, predominantly membranous S100A14 expression mainly in the epithelial compartment. (C) Representative OSCC (early invasive) lesion showing a gradient of S100A14 immunostaining: central area (C1) shows a strong, membranous staining in contrast to a very weak, cytoplasmic staining in the invading front area (C2). (D) Representative OSCC (advanced invasive) specimen showing mixed membranous and cytoplasmic staining of S100A14 in the more superficial invading islands (D1) compared to the weak, predominantly cytoplasmic staining in the deep invading tumour islands (D2).

Table 1 – Semiquantitative evaluation of the S100A14 localisation in invading islands of the OSCCs.

% of +ve cells	Mem. *n* (%)	Mem.+Cyto. *n* (%)	Cyto. *n* (%)
Low score (0–9%)	10 (62.5)	0 (0)	6 (37.5)
Moderate score (10–49%)	6 (37.5)	7 (43.75)	9 (56.25)
High score (50–100%)	0 (0)	9 (56.25)	1 (6.25)

Mem., membranous; Cyto., Cytoplasmic.

mixed membranous and cytoplasmic staining as well. None of the epithelial cells showed nuclear staining. All of the ODLs were positive for S100A14 and the expression pattern was similar to that found in NHOM (Fig. 1B). However, the staining intensity was heterogenous across the ODL specimens, with some tissue specimens displaying a weaker or a stronger staining for S100A14 than NHOM. In the OSCC specimens, S100A14 expression was variable across the different areas of the same OSCC lesion. Expression was very weak or absent in invading islands of tumour cells (poorly differentiated areas/islands) compared to central areas including the surface/superficial epithelial layers (more differentiated areas) of the OSCC specimens (Fig. 1C). Of note, there was a change in the sub-cellular localisation of the S100A14 protein from plasma membrane to cytoplasm in the invading islands of tumour cells when compared to the predominantly membranous staining seen in the central areas of the OSCCs (Figs. 1C and D). Semiquantitative evaluation of S100A14 sub-cellular localisation in the invading islands of OSCCs revealed three different expression patterns (only membranous, mixed membranous and cytoplasmic or only cytoplasmic localisation) (Table 1). Nine of the OSCC specimens (56.25%) showed *high score* mixed membranous and cytoplasmic staining compared to 6 OSCCs (37.5%) with *moderate score* membranous staining in the invading islands (Table 1). No staining was found in the connective tissue cells, except occasional plasma cells which showed a strong cytoplasmic staining. No correlation was found between the expression patterns of S100A14 found in OSCCs with the available clinical parameters (TNM stage, tumour differentiation and location).

3.2. *S100A14 mRNA is gradually down-regulated in an in vitro OSCC progression model, with invasive OSCC cell-lines expressing the least amount of S100A14 mRNA*

The mean expression of *S100A14* mRNA was found to be gradually down-regulated during the transition from normal oral keratinocytes to dysplastic (30% decrease, $P > 0.05$) and OSCC derived cell-lines (85% decrease, $P < 0.001$) (Fig. 2A). Moreover, there was a significant decrease of *S100A14* mRNA expression during the transition from dysplastic to OSCC derived cell-lines (79% decrease, $P < 0.05$) (Fig. 2A). Amongst the normal keratinocytes examined, similar expression of *S100A14* mRNA was found (Fig. 2B). Dysplastic cells, however, demonstrated variable amounts of *S100A14* mRNA, with POE9n (mortal cell-line) expressing more and D20 and DOK (immortal cell-lines) expressing less *S100A14* mRNA levels (Fig. 2B). *S100A14* mRNA expression was relatively low in most of the carcinoma derived cell-lines examined. Interestingly, more invasive OSCC derived cells like VB6, H357 and SCC25 expressed little or no *S100A14* mRNA (Fig. 2B).

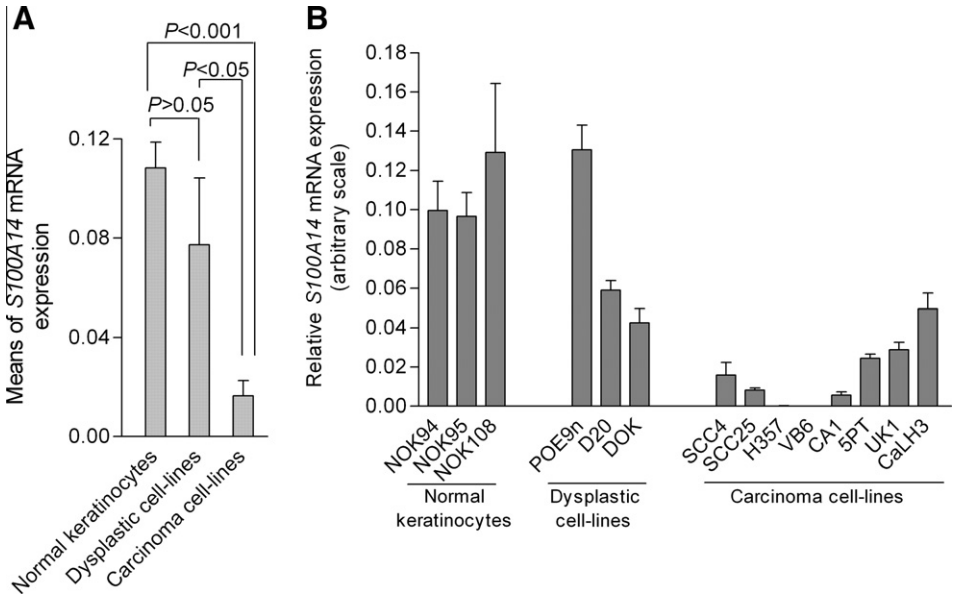

Fig. 2 – Gradual down-regulation of *S100A14* mRNA in the *in vitro* OSCC progression model. (A) Mean *S100A14* mRNA expression, as determined by qRT-PCR, is progressively down-regulated during the transition from normal to dysplastic and cancer stages in an *in vitro* OSCC progression model. Error bars represent SD. ANOVA with Bonferroni *post-hoc* tests was used for statistical analysis. (B) Invasive cell lines (VB6, H357 and SCC25) expressed low/no *S100A14* mRNA. *S100A14* mRNA expression was normalised with expression of *GAPDH* mRNA. Error bars represent SD of three technical replicates.

3.3. *S100A14 expression vector and siRNA targeting S100A14 successfully modulate endogenous S100A14 mRNA and protein levels in CaLH3 and H357 cell-lines*

S100A14-CaLH3 and S100A14-H357 cells expressed significantly higher *S100A14* mRNA and protein levels compared to the control-CaLH3 and control-H357 cells (Figs. 3A and B). Similarly, *S100A14* mRNA and protein levels were significantly decreased in the S100A14-siRNA cells compared to the sc-siRNA cells (Figs. 3C and D).

3.4. *S100A14 regulates invasiveness of CaLH3 and H357 cell-lines in vitro*

The effect of S100A14 protein on cell invasion was examined using *in vitro* Matrigel invasion assay. A significantly lower number of S100A14-CaLH3 cells invaded through the Matrigel (ECM equivalent) compared to the control-CaLH3 cells ($P = 0.039$) (Figs. 4A and D). Similarly, invasive potential of S100A14-H357 cells was also suppressed when compared to the control-H357 cells ($P = 0.066$) (Figs. 4B and D). On contrary, significantly higher number of S100A14-siRNA cells invaded through the Matrigel compared to the sc-siRNA cells ($P = 0.011$) (Figs. 4C and D).

3.5. *S100A14 over-expression is associated with down-regulation of MMP1 and MMP9 mRNA expression in CaLH3 and H357 cell-lines*

PCR array was used to examine differentially expressed invasion and metastasis related genes associated with S100A14 over-expression. S100A14-CaLH3 replicates clustered separately from the replicates of control-CaLH3 cells when using unsupervised hierarchical clustering (Fig. 5A). SAM analysis revealed significant (FDR = 0) down-regulation of invasion and metastasis promoting genes, such as *MMP1, MMP9, FN1, CD44* and *TNC* in S100A14-CaLH3 compared to control-CaLH3 cells (Table 2). Independent validation of the differentially expressed genes, as identified by PCR array, was done by performing qRT-PCR using TaqMan assays for *MMP1, MMP9, FN1* and *CD44* genes. Consistent with the PCR array results, *MMP1* ($P = 0.045$, 20-folds down-regulation) and *MMP9* ($P = 0.006$, 12-folds down-regulation), *FN1* ($P = 0.003$, 4.9-folds down-regulation) and *CD44* ($P = 0.004$, 1.7-folds down-regulation) (*FN1*and *CD44* data not shown) were found to be significantly down-regulated in S100A14-CaLH3 cells (Fig. 5B, upper panel). In parallel with the S100A14-CaLH3 cells, *MMP1* ($P = 0.0003$, 2.5-folds down-regulation) and *MMP9* ($P = 0.0002$, 3-folds down-regulation) mRNA levels were also significantly

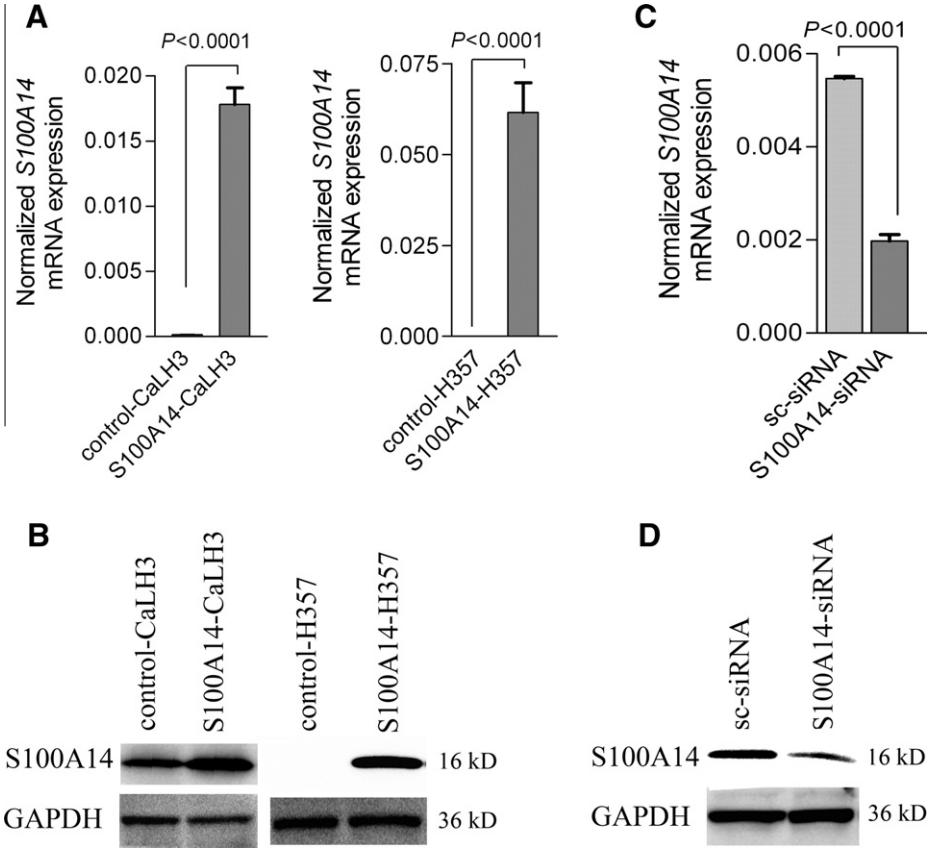

Fig. 3 – Modulation of endogenous *S100A14* mRNA and protein levels by S100A14 expression vector and siRNA targeting S100A14 in CaLH3 and H357 cell-lines. S100A14-CaLH3 and S100A14-H357 cells show significantly high *S100A14* transcripts (A) and protein (B) compared to that of the control-CaLH3 and control-H357 cells. Conversely, S100A14-siRNA cells express significantly less *S100A14* mRNA (C) and protein levels (D) compared to that of the sc-siRNA cells. *GAPDH* mRNA was used to normalise expression of *S100A14* mRNA in qRT-PCR. Error bars represent SEM of three biological replicates done in triplicates in (A) and SD of three technical replicates in (C). Student's-*t* test was used for statistical analysis.

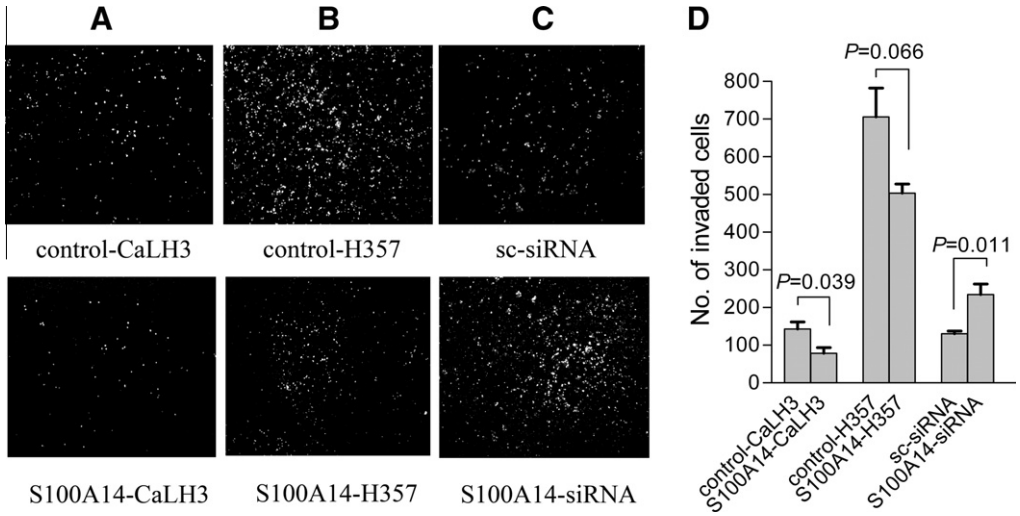

Fig. 4 – Regulation of invasive phenotype of CaLH3 and H357 cell-lines by S100A14. Effect of S100A14 over-expression in CaLH3 and H357 cell-lines (A, B) and knock-down in CaLH3 cell-line (C) on invasive behaviour was examined *in vitro* by Matrigel invasion assay. 1×10^5 cells/well were seeded on the Transwell insert (8 μm pore size, BD Falcon™) coated with 20 μg of Matrigel (354230, BD Biosciences, MA, USA). After incubation at 37 °C for 20 h, the invaded cells were fixed with 4% PFA, stained with DAPI and analysed by fluorescence microscopy (4× magnification, Nikon TR200 fluorescence microscope). Photomicrographs show DAPI stained nuclei of the invaded cells (original magnification 4×). (D) Numbers of DAPI stained invaded cells were quantified by using ImageJ software. Error bars represents SEM of quadruplicate assays. Student's-t test was used for statistical analysis.

down-regulated in S100A14-H357 compared to the control-H357 cells (Fig. 5B, lower panel). In addition, proteolytic activity of MMP9 was found to be suppressed in S100A14-CaLH3 cells compared to control-CaLH3 cells (Fig. 5C). However, MMP9 activity could not be detected for both control-H357 and S100A14-H357 cells (Fig. 5C).

3.6. *MMP1and MMP9 mRNA levels are inversely correlated with the S100A14 mRNA levels in OSCC specimens*

In vivo relevance of down-regulation of *MMP1* and *MMP9* mRNA by S100A14 over-expression in CaLH3 and H357 cell-lines was tested by examining co-expression *S100A14* *MMP1* and *MMP9* mRNA levels in 19 cases of OSCCs. A significantly inverse correlation ($r = -0.69$, $p = 0.0009$) was found between the mRNA ratios of *S100A14* (OSCCs/normal controls) and *MMP1* (OSCCs/normal controls) (Fig. 6A). Similarly, *MMP9* mRNA expression was also negatively correlated ($r = -0.45$, $p = 0.053$) with the *S100A14* mRNA expression (Fig. 6B).

4. Discussion

This study demonstrates that S100A14 regulates the invasive phenotype of oral carcinoma derived CaLH3 and H357 cell-lines and this regulation is associated with the modulation of key genes involved in invasion and metastasis, in particular *MMP1* and *MMP9*. Previously we found down-regulated expression of *S100A14* mRNA in OSCC tissues compared to their pair-wised normal controls.[9] Assessment of the *in vivo* specimens in this study further confirmed the down-regulation of S100A14 protein in OSCCs, particularly in the invasive tumour islands (Fig. 1). These *in vivo* data were mirrored by the *in vitro* data obtained in an experimental progressive model of oral carcinogenesis (Fig. 2). Taken together, these findings suggest that reduced expression of S100A14 might be related to OSCC progression and might influence the invasive phenotype of the tumour cells. We found membranous to cytoplasmic translocation of the S100A14 protein from highly differentiated (central/superficial) areas in the OSCCs to the poorly differentiated (invading islands of tumour cells) areas, which might indicate an association of S100A14 with cell differentiation. In fact, similar observations supporting this suggestion have been previously reported in tonsil squamous cell carcinoma and bladder papillary transitional cell carcinoma.[23] However, a significant correlation between the expression status of S100A14 and the degree of tumour differentiation or other clinical parameters like TNM stage and tumour location could not be detected in the present study, possibly due to the relatively small number of the OSCC cases examined. Nevertheless, a recent study has reported a correlation between decreased S100A14 immunoexpression and poor differentiation and high metastatic potential of colorectal cancers.[24] Overall, reduced expression with membrane to cytoplasmic switch of the S100A14 might be related to the invasive phenotype of tumour cells.

A role for S100A14 in the regulation of invasive phenotype of tumour cells was also substantiated in the experimental part of the current study. Retroviral vector mediated over-expression of S100A14 resulted in suppression of CaLH3 and H357 cell invasion, and conversely, siRNA mediated knock-down of S100A14 led to an increase in invasion of CaLH3 cells through Matrigel, an *in vitro* equivalent of ECM (Fig. 4). These findings indicate that change in the endogenous S100A14 expression levels might influence the invasive phenotype of tumour cells. This suggestion has been supported by the

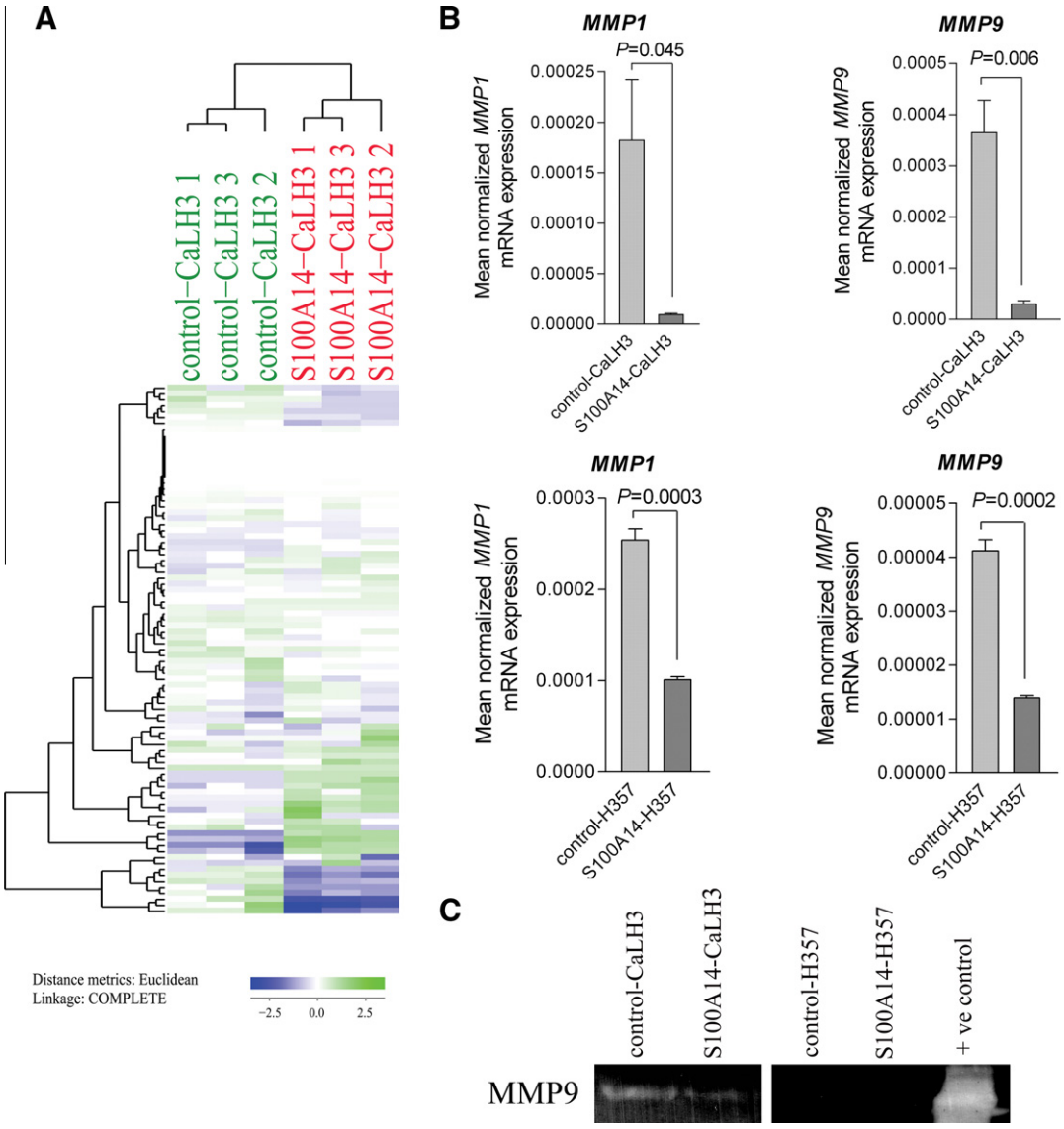

Fig. 5 – Modulation of genes involved in invasion and metastasis by S100A14 over-expression. Based on overall expression status of the 84 genes related to invasion and metastasis, unsupervised hierarchical cluster analysis was performed. Replicates of S100A14-CaLH3 cells have clustered separately compared to that of the control-CaLH3 cells. (B) Array results for *MMP1* and *MMP9* genes modulated by S100A14 over-expression were independently validated in CaLH3 (upper panel) and H357 (lower panel) cell-lines using qRT-PCR (TaqMan). Error bar represents SEM of three biological replicates done in triplicates. Student's-t test was used for statistical analysis. (C) Representative image showing gelatinolytic activity of MMP9. + ve control: conditioned serum-free medium from THP-1 cells.

findings that reduced S100A14 expression was associated with the invasive islands of the tumour cells in OSCC specimens *in vivo* (Fig. 1C and D) and the more invasive OSCC cell-lines (VB6, H357 and SCC25) *in vitro* (Fig. 2B). Unsupervised hierarchical cluster analysis of the PCR array data revealed a distinct mRNA profile of the genes involved in invasion and metastasis in S100A14-CaLH3 compared to control-CaLH3 cells (Fig. 5A), indicating a role for S100A14 in regulating the expression of these genes. SAM analysis further identified a number of invasion and metastasis promoting genes like *MMP1*, *MMP9*, *FN1*, *CD44* and *TNC* to be significantly down-regulated in the S100A14-CaLH3 cells (Table 2). *MMP1* and *MMP9*, the highly responsive genes to S100A14 over-expression in CaLH3 cells, were also found to be significantly down-regulated in H357 cell-line when S100A14 was over-expressed (Fig. 5B, lower panel). In parallel, suppression of MMP9 proteolytic activity was also found in S100A14-CaLH3 cells (Fig. 5C). Absence of MMP9 proteolytic activity observed for control-H357 and S100A14-H357 cells might be due to undetectable amount of secreted MMP9 in the culture medium. Overall, these findings indicate that *MMP1* and *MMP9* are amongst the key downstream targets of S100A14 and their negative regulation by S100A14 might contribute to the suppression of invasive potential of CaLH3 and H357 cell-lines. This suggestion has also been reflected in the OSCC specimens *in vivo* where *MMP1* and MMP9 mRNA levels were

Table 2 – List of candidate invasion and metastasis related genes modulated by S100A14 over-expression in CaLH3 cell-line.

UniGene	Ref Seq	Gene symbol	Description	Fold change
Down-regulated genes by S100A14 over-expression				
Hs.83169	NM_002421	*MMP1*	Matrix metallopeptidase 1 (interstitial collagenase)	−12.63
Hs.523446	NM_080629	*COL11A1*	Collagen, type XI, alpha 1	−9.10
Hs.297413	NM_004994	*MMP9*	Matrix metallopeptidase 9 (gelatinase B, 92 kDa gelatinase, 92 kDa type IV collagenase)	−8.38
Hs.203717	NM_002026	*FN1*	Fibronectin 1	−4.33
Hs.143250	NM_002160	*TNC*	Tenascin C (hexabrachion)	−3.15
Hs.409034	NM_001855	*COL15A1*	Collagen, type XV, alpha 1	−2.71
Hs.502328	NM_000610	*CD44*	CD44 molecule (Indian blood group)	−2.20
Up-regulated genes by S100A14 over-expression				
Hs.2936	NM_002427	*MMP13*	Matrix metallopeptidase 13 (collagenase 3)	8.10
Hs.81071	NM_004425	*ECM1*	Extracellular matrix protein 1	5.45
Hs.172631	NM_000632	*ITGAM*	Integrin, alpha M (complement component 3 receptor 3 subunit)	4.77
Hs.371199	NM_003919	*SGCE*	Sarcoglycan, epsilon	2.71
Hs.694732	NM_000885	*ITGA4*	Integrin, alpha 4 (antigen CD49D, alpha 4 subunit of VLA-4 receptor)	2.69
Hs.172928	NM_000088	*COL1A1*	Collagen, type I, alpha 1	2.50
Hs.633514	NM_003255	*TIMP2*	TIMP metallopeptidase inhibitor 2	2.40

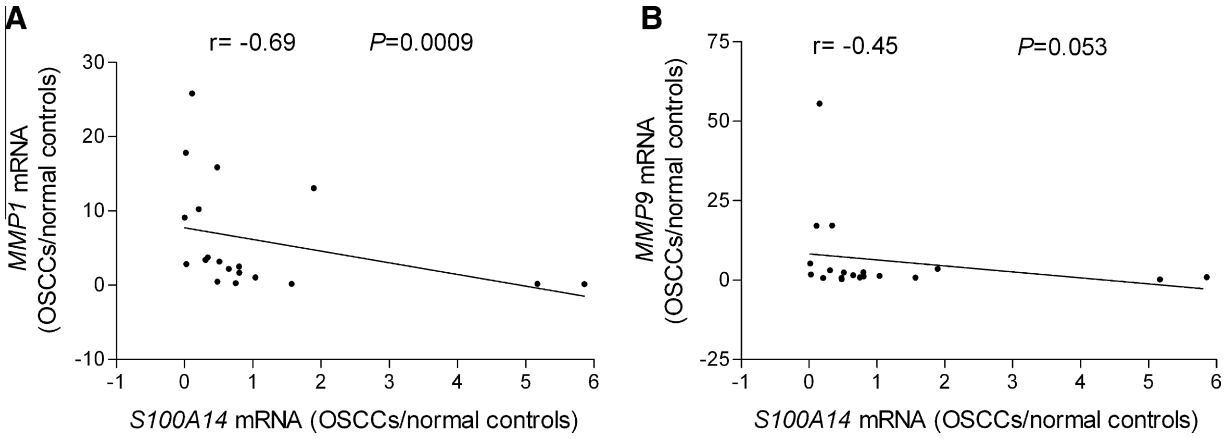

Fig. 6 – Inverse correlation of *MMP1* and *MMP9* mRNA levels with *S100A14* mRNA level in OSCCs. *S100A14*, *MMP1*and *MMP9* mRNA expression levels were calculated using qRT-PCR (using relative standard curve method). OSCC/normal control ratios of the normalised *MMP1* and *MMP9* mRNA levels were correlated with *S100A14* mRNA level using Spearmen's correlation analysis.

inversely correlated with the *S100A14* mRNA level (Fig. 6). Over-expression of MMP1 and MMP9 has been shown to be associated with high metastatic potential and poor clinical outcomes in oral cancers.[41–43] Taken together, it can be speculated that one way of transformed cells to acquire an invasive phenotype might be through the up-regulation of *MMP9* and *MMP1*, perhaps by down-regulating S100A14 expression and this points towards a tumour suppressive role for S100A14. On the other hand, MMP13, another member of the MMP family associated as well with invasion and aggressiveness of OSCC,[44,45] was unexpectedly found to be over-expressed in S100A14-CaLH3 cells (Table 2). Nevertheless, there are previous reports which are in line with our observation, showing that MMP13 was down- and MMP9 and MMP2 were up-regulated in a highly invasive αvβ6 over-expressing VB6 cell-line (OSCC derived cell-line), suggesting that MMP13 might have a different function in tumour progression.[46,47] Further investigations are therefore necessary to clarify the role of MMP13 in S100A14-mediated modulation of oral cancer invasion.

Sub-cellular localisation of a protein has often been considered to provide clues to its function.[48] Although investigating the underlying molecular mechanism for modulation of *MMP1* and *MMP9* expression by S100A14 over-expression was not the focus of this study, it can be suggested that S100A14 might modulate the mRNA signature of these genes by signal transduction mechanism since S100A14 was found to be predominantly localised in the plasma membrane in the majority of archival tissues examined and in the S100A14-CaLH3 and S100A14-H357 cells (data not shown). In support for this suggestion are previous findings showing interactions between S100A14 and nucleobindin protein.[23] Nucleobindin has been suggested to be involved in G protein-coupled signal transduction in a calcium dependent manner.[49] In addition, presence of N-myristoylation site at the N-terminus of S100A14 protein suggests that S100A14

can interact with other membrane receptors potentially involved in signal transduction.[22] Nevertheless, membrane to cytoplasmic translocation of the S100A14 found in invading islands of the OSCC specimens and its significance in signal transduction mechanism warrants further investigation.

In conclusion, our results indicate a novel role of S100A14 in tumour invasion. The data presented here demonstrate that loss of S100A14 expression is associated with the invasive phenotype of OSCC cells *in vivo* and *in vitro*. Additionally, we show that *in vitro* modulation of the endogenous S100A14 expression is associated with subsequent change in invasive phenotype of OSCC cell-lines with concomitant modulation of expression and activity of *MMP1* and *MMP9*. Together with our previous findings related to involvement of S100A14 in regulation of cell proliferation by inducing G1-phase cell cycle arrest, the data of the current study suggest that S100A14 might be involved in multiple biological processes relevant for human carcinogenesis, in particular OSCCs. Further characterisation of the regulation and function of S100A14 might contribute to the better understanding of oral carcinogenesis.

Conflict of interest statement

None declared.

Acknowledgements

We are grateful to Dr. Oleg Tsinkalovsky for assistance with the cell sorting and Mrs. Gunnvor Øijordsbakken for excellent technical assistance. This study was supported by the Norwegian State Educational Loan Fund (Quota Programme, DS), Meltzer's fund (project no: 803172, DS) and NFR (project no: 178601, DEC).

Appendix A. Supplementary data

Supplementary data associated with this article can be found, in the online version, at doi:10.1016/j.ejca.2010.10.012.

REFERENCES

1. Silverman SJ. Demographics and occurrence of oral and pharyngeal cancers: the outcomes, the trends, the challenge. *J Am Dent Assoc* 2001;**132**:7S–11S.
2. Massano J, Regateiro FS, Januário G, Ferreira A. Oral squamous cell carcinoma: review of prognostic and predictive factors. *Oral Surg Oral Med Oral Pathol Oral Radiol Endod* 2006;**102**:67–76.
3. Woolgar JA. Histopathological prognosticators in oral and oropharyngeal squamous cell carcinoma. *Oral Oncol* 2006;**42**:229–39.
4. Steeg PS. Tumor metastasis: mechanistic insights and clinical challenges. *Nat Med* 2006;**12**:895–904.
5. Cairns RA, Khokha R, Hill RP. Molecular mechanisms of tumor invasion and metastasis: an integrated view. *Curr Mol Med* 2003;**3**:659–71.
6. Donato R. S100: a multigenic family of calcium-modulated proteins of the EF-hand type with intracellular and extracellular functional roles. *Int J Biochem Cell Biol* 2001;**33**:637–68.
7. Marenholz I, Heizmann CW, Fritz G. S100 proteins in mouse and man: from evolution to function and pathology (including an update of the nomenclature). *Biochem Biophys Res Commun* 2004;**322**:1111–22.
8. Salama I, Malone PS, Mihaimeed F, Jones JL. A review of the S100 proteins in cancer. *Eur J Surg Oncol* 2008;**34**:357–64.
9. Sapkota D, Bruland O, Bøe OE, et al. Expression profile of the S100 gene family members in oral squamous cell carcinomas. *J Oral Pathol Med* 2008;**37**:607–15.
10. Ji J, Zhao L, Wang X, et al. Differential expression of S100 gene family in human esophageal squamous cell carcinoma. *J Cancer Res Clin Oncol* 2004;**130**:480–6.
11. Yao R, Lopez-Beltran A, Maclennan GT, et al. Expression of S100 protein family members in the pathogenesis of bladder tumors. *Anticancer Res* 2007;**27**:3051–8.
12. Saleem M, Kweon M-H, Johnson JJ, et al. S100A4 accelerates tumorigenesis and invasion of human prostate cancer through the transcriptional regulation of matrix metalloproteinase 9. *Proc Natl Acad Sci USA* 2006;**103**:14825–30.
13. Bulk E, Sargin B, Krug U, et al. S100A2 induces metastasis in non-small cell lung cancer. *Clin Cancer Res* 2009;**15**:22–9.
14. Whiteman HJ, Weeks ME, Dowen SE, et al. The role of S100P in the invasion of pancreatic cancer cells is mediated through cytoskeletal changes and regulation of cathepsin D. *Cancer Res* 2007;**67**:8633–42.
15. Pierce A, Barron N, Linehan R, et al. Identification of a novel, functional role for S100A13 in invasive lung cancer cell lines. *Eur J Cancer* 2008;**44**:151–9.
16. Bjornland K, Winberg JO, Odegaard OT, et al. S100A4 involvement in metastasis: deregulation of matrix metalloproteinases and tissue inhibitors of matrix metalloproteinases in osteosarcoma cells transfected with an anti-S100A4 ribozyme. *Cancer Res* 1999;**59**:4702–8.
17. Qin F, Song Y, Li Z, et al. S100A8/A9 induces apoptosis and inhibits metastasis of CasKi human cervical cancer cells. Pathol Oncol Res 2009. doi:10.1007/s12253-009-9225-2.
18. Egeblad M, Werb Z. New functions for the matrix metalloproteinases in cancer progression. *Nat Rev Cancer* 2002;**2**:161–74.
19. Björklund M, Koivunen E. Gelatinase-mediated migration and invasion of cancer cells. *Biochim Biophys Acta* 2005;**1755**:37–69.
20. Thomas GT, Lewis MP, Speight PM. Matrix metalloproteinases and oral cancer. *Oral Oncol* 1999;**35**:227–33.
21. Werner JA, Rathcke IO, Mandic R. The role of matrix metalloproteinases in squamous cell carcinomas of the head and neck. *Clin Exp Metastasis* 2002;**19**:275–82.
22. Pietas A, Schlüns K, Marenholz I, et al. Molecular cloning and characterization of the human S100A14 gene encoding a novel member of the S100 family. *Genomics* 2002;**79**:513–22.
23. Adam PJ, Boyd R, Tyson KL, et al. Comprehensive proteomic analysis of breast cancer cell membranes reveals unique proteins with potential roles in clinical cancer. *J Biol Chem* 2003;**278**:6482–9.
24. Wang HY, Zhang JY, Cui JT, et al. Expression status of S100A14 and S100A4 correlates with metastatic potential and clinical outcome in colorectal cancer after surgery. *Oncol Rep* 2010;**23**:45–52.
25. Costea DE, Loro LL, Dimba EAO, Vintermyr OK, Johannessen AC. Crucial effects of fibroblasts and keratinocyte growth factor on morphogenesis of reconstituted human oral epithelium. *J Invest Dermatol* 2003;**121**:1479–86.
26. Dysvik B, Vasstrand EN, Løvlie R, et al. Gene expression profiles of head and neck carcinomas from Sudanese and Norwegian patients reveal common biological pathways regardless of race and lifestyle. *Clin Cancer Res* 2006;**12**:1109–20.

27. Rheinwald JG, Hahn WC, Ramsey MR, et al. A two-stage, p16INK4A- and p53-dependent Keratinocyte senescence mechanism that limits replicative potential independent of telomere status. *Mol Cell Biol* 2002;**22**:5157–72.
28. McGregor F, Muntoni A, Fleming J, et al. Molecular changes associated with oral dysplasia progression and acquisition of immortality: potential for its reversal by 5-azacytidine. *Cancer Res* 2002;**62**:4757–66.
29. Chang SE, Foster S, Betts D, Marnock WE. DOK, a cell line established from human dysplastic oral mucosa, shows a partially transformed non-malignant phenotype. *Int J Cancer* 1992;**52**:896–902.
30. Rheinwald JG, Beckett MA. Tumorigenic keratinocyte lines requiring anchorage and fibroblast support cultured from human squamous cell carcinomas. *Cancer Res* 1981;**41**:1657–63.
31. Prime SS, Nixon SV, Crane IJ, et al. The behaviour of human oral squamous cell carcinoma in cell culture. *J Pathol* 1990;**160**:259–69.
32. Thomas GJ, Lewis MP, Whawell SA, et al. Expression of the αvβ6 integrin promotes migration and invasion in squamous carcinoma cells. *J Invest Dermatol* 2001;**117**:67–73.
33. Mackenzie IC. Growth of malignant oral epithelial stem cells after seeding into organotypical cultures of normal mucosa. *J Oral Pathol Med* 2004;**33**:71–8.
34. Harper LJ, Piper K, Common J, Fortune F, Mackenzie IC. Stem cell patterns in cell lines derived from head and neck squamous cell carcinoma. *J Oral Pathol Med* 2007;**36**:594–603.
35. Costea DE, Lukandu O, Bui L, et al. Adverse effects of Sudanese toombak vs. Swedish snuff on human oral cells. *J Oral Pathol Med* 2009;**39**:128–40.
36. Gjerdrum C, Tiron C, Høiby T, et al. Axl is an essential epithelial-to-mesenchymal transition-induced regulator of breast cancer metastasis and patient survival. *Proc Natl Acad Sci USA* 2010;**107**:1124–9.
37. Dysvik B, Jonassen I. J-Express: exploring gene expression data using Java. *Bioinformatics* 2001;**17**:369–70.
38. Tusher VG, Tibshirani R, Chu G. Significance analysis of microarrays applied to the ionizing radiation response. *Proc Natl Acad Sci USA* 2001;**98**:5116–21.
39. Muller PY, Janovjak H, Miserez AR, Dobbie Z. Processing of gene expression data generated by quantitative real-time RT-PCR. *Biotechniques* 2002;**32**:1372–4 [6, 8–9].
40. Gharagozlian S, Svennevig K, Bangstad H-J, Winberg J-O, Kolset S. Matrix metalloproteinases in subjects with type 1 diabetes. *BMC Clin Pathol* 2009;**9**:7.
41. Ye H, Yu T, Temam S, et al. Transcriptomic dissection of tongue squamous cell carcinoma. *BMC Genomics* 2008;**9**:69.
42. Mitra RS, Goto M, Lee JS, et al. Rap1GAP promotes invasion via induction of matrix metalloproteinase 9 secretion, which is associated with poor survival in low N-stage squamous cell carcinoma. *Cancer Res* 2008;**68**:3959–69.
43. Jordan RCK, Macabeo-Ong M, Shiboski CH, et al. Overexpression of matrix metalloproteinase-1 and -9 mRNA is associated with progression of oral dysplasia to cancer. *Clin Cancer Res* 2004;**10**:6460–5.
44. Marjaana L, Pia V, Pauliina K, et al. Association between high collagenase-3 expression levels and poor prognosis in patients with head and neck cancer. *Head Neck* 2006;**28**:225–34.
45. Johansson N, Airola K, Grenman R, et al. Expression of collagenase-3 (matrix metalloproteinase-13) in squamous cell carcinomas of the head and neck. *Am J Pathol* 1997;**151**:499–508.
46. Ylipalosaari M, Thomas GJ, Nystrom M, et al. [alpha]v[beta]6 integrin down-regulates the MMP-13 expression in oral squamous cell carcinoma cells. *Exp Cell Res* 2005;**309**:273–83.
47. Gareth JT, Mark PL, Ian RH, John FM, Paul MS. Alphavbeta6integrin promotes invasion of squamous carcinoma cells through up-regulation of matrix metalloproteinase-9. *Int J Cancer* 2001;**92**:641–50.
48. Horton P, Park K-J, Obayashi T, et al. WoLF PSORT: protein localization predictor. *Nucleic Acids Res* 2007;**35**:W585–7.
49. Lin P, Fischer T, Weiss T, Farquhar MG. Calnuc, an EF-Hand Ca^{2+} binding protein, specifically interacts with the C-terminal alpha5-helix of G(alpha)i3. *Proc Natl Acad Sci USA* 2000;**97**:674–9.